Volume 1 | Number 1 | Jan 2013 | Pages 1–100

ChemComm

Chemical Communications
www.rsc.org/chemcomm

ROYAL SOCIETY OF CHEMISTRY

This is an *Accepted Manuscript*, which has been through the Royal Society of Chemistry peer review process and has been accepted for publication.

Accepted Manuscripts are published online shortly after acceptance, before technical editing, formatting and proof reading. Using this free service, authors can make their results available to the community, in citable form, before we publish the edited article. We will replace this *Accepted Manuscript* with the edited and formatted *Advance Article* as soon as it is available.

You can find more information about *Accepted Manuscripts* in the **Information for Authors**.

Please note that technical editing may introduce minor changes to the text and/or graphics, which may alter content. The journal's standard **Terms & Conditions** and the **Ethical guidelines** still apply. In no event shall the Royal Society of Chemistry be held responsible for any errors or omissions in this *Accepted Manuscript* or any consequences arising from the use of any information it contains.

Journal Name

COMMUNICATION

Multifaceted chelating μ-(η³:η³-*antifacial*)-(*cis*-C₄R₂H₂) coordination motif in binuclear complexes†

Cham-Chuen Liu, Michael C. W. Chan,* Po-Kam Lo, Kai-Chung Lau* and Shek-Man Yiu

The novel μ-C₄R₂H₂ core structure (formed by an unprecedented regioselective, redox-neutral C(sp²)–C(sp²) coupling process) in binuclear group 4 complexes displays adaptable coordination and accommodates different metal sizes, and is sufficiently robust to promote interesting catalytic reactivity at the bimetallic centers.

The search for novel organometallic ligand systems continues to motivate research endeavors. For binuclear complexes, unsaturated carbon-based bridging ligands that can exhibit variable hapticity (reduced to facilitate substrate binding or increased to support hitherto unstable species) and redox-active behavior (to promote and tolerate different oxidation states and electronic requirements), and can potentially mediate attractive reactivity and catalytic transformations (e.g. metal-metal synergistic and cooperative effects[1]), are of interest. In this work, the unusual delocalized μ-(C₄R₂H₂) ligand core is formally dianionic and a 6-electron donor. Related auxiliaries such as the 2,2′-bipyridyl dianion in $[μ-(η^4:η^4)-(bipyridyl)-Y_2]$,[2] μ-(*trans*-butatriene) in $[μ-(C_4H_4)-Ti_2]$,[3] and the isomeric trimethylenemethane, TMM in $[μ-(η^3:η^3)-(C(CH_2)_3)-Ln_2]$,[4,5] are known in the literature. However, these ligands do not contain additional chelating sites and are prone to undergo transformation (e.g. by electrophilic attack) and subsequent displacement, and this is reflected by a dearth of catalytic applications. Here, we demonstrate that by exploiting the chelate effect and attendant steric protection, the bis-(phenolate-pyridine)-(μ-C₄R₂H₂) framework can support interesting catalytic reactivity at the bimetallic sites.

Our ongoing studies concerning group 4 organometallics indicated that, compared with chelating σ-aryl ligands,[6,7] the σ-alkenyl moiety can offer greater flexibility and π-donation. The metalation of the vinyl ligand H₂L^H (R = H) with M(CH₂Ph)₄ in pentane/Et₂O yielded black-purple (Ti) and deep orange (Zr and Hf) crystalline products, while for H₂L^Me (R = Me), intensely dark turquoise (Zr) and dark

indigo (Hf) crystalline solids were obtained (Scheme 1).[8] These colors are reminiscent of d¹ compounds (e.g. ZrCl₃ exists as blue-black solid), but all products were found to be diamagnetic. The surprising nature of the products were elucidated by X-ray crystallography for **Ti₂^H**, **Zr₂^H** and **Hf₂^Me** (Figure 1). The dimeric, racemic molecular structures depict a bis-[O,N]-chelating μ-(η³:η³-*antifacial*)-(*cis*-C₄R₂H₂) framework that coils around and binds the two metals on opposite faces of the delocalized C₄ moiety.

While the M–C(η³) bond lengths[9] are varied (av. 2.427, 2.566, 2.565 Å respectively), it is particularly striking that the M-C₄-M coordination is dissimilar (see Table 1 for illustration); for example, the M1 atom in both **Ti₂^H** and **Zr₂^H** is closest to C4 followed by C3, and weakly bound by C2, but the Hf1 atom in **Hf₂^Me** is closest to C2 and weakly coordinated to C1 and C3. Conversely, the geometry of the C₄ core is consistent and relatively independent of the metal; the C–C distances (1.409(3)–1.446(5) Å) may be considered equivalent within experimental error, and the C–C–C angles (av. 128.1–133.0°) and torsion angle (24.6–30.3°) show only minor differences. The M–C(η³) distances in **Ti₂^H**, **Zr₂^H** and **Hf₂^Me** (2.335(2)–2.700(2) Å) are generally longer than the M–C(sp²) bonds in mononuclear σ-aryl congeners (M = Ti–Hf: 2.15–2.35 Å),[7] but shorter than those in the μ-TMM relatives $[(C_5Me_5)_2Ln]_2[μ-(η^3:η^3)-(C(CH_2)_3)]$ containing larger Ln³⁺ ions (La, Pr, Sm; 2.546(4)–2.870(5) Å).[4] In contrast, the C–C distances reported for the TMM ligand (1.406(9)–1.432(6) Å) are remarkably similar to those for the μ-C₄R₂H₂ core.
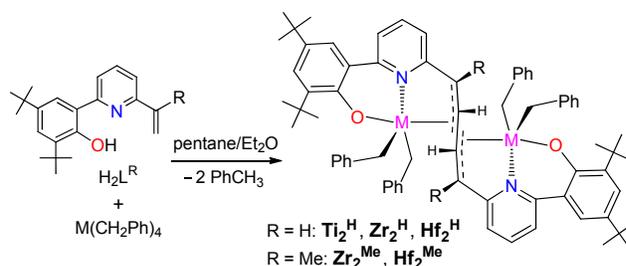
Scheme 1 Synthesis of binuclear complexes **M₂^R**.

Department of Biology and Chemistry, City University of Hong Kong, Tat Chee Avenue, Kowloon, Hong Kong, China. Email: mcwchan@cityu.edu.hk; kaichung@cityu.edu.hk
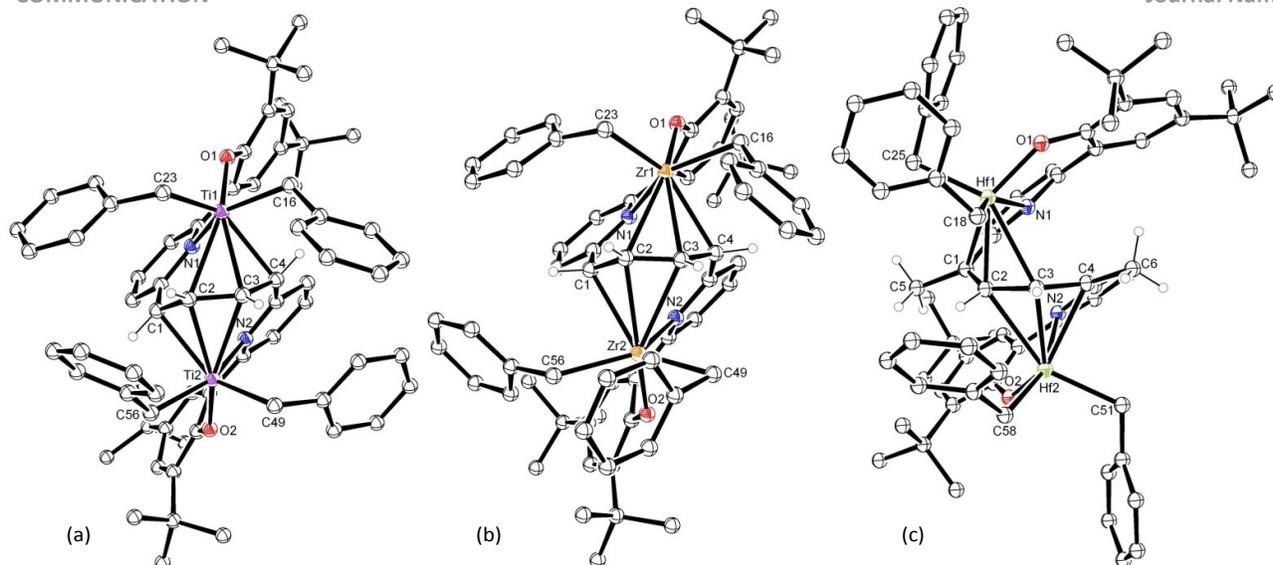
Figure 1 Perspective views (30% probability ellipsoids; key atoms labeled and H shown for μ-C$_4$ unit only) of **Ti$_2$^{H}** (a), **Zr$_2$^{H}** (b) and **Hf$_2$^{Me}** (c).

Table 1 Selected bond lengths (Å; square parentheses signify non-bonded distances) and angles (°) for **Ti$_2$^{H}**, **Zr$_2$^{H}** and **Hf$_2$^{Me}**

	Ti$_2$^{H}	Zr$_2$^{H}	Hf$_2$^{Me}
C1–C2 (Å)	1.438(3)	1.434(4)	1.435(4)
C2–C3 (Å)	1.409(3)	1.412(4)	1.442(5)
C3–C4 (Å)	1.432(3)	1.428(4)	1.446(5)
M1–C1, M2–C4 (Å)	[3.161(2), 3.140(2)]	[3.187(2), 3.270(3)]	2.640(3), 2.571(3)
M1–C2, M2–C3 (Å)	2.553(2), 2.552(2)	2.665(3), 2.700(2)	2.431(3), 2.413(3)
M1–C3, M2–C2 (Å)	2.378(2), 2.396(2)	2.533(2), 2.532(3)	2.651(3), 2.684(3)
M1–C4, M2–C1 (Å)	2.335(2), 2.349(2)	2.461(3), 2.507(2)	[3.437(3), 3.460(3)]
C1–C2–C3 (°)	128.9(2)	129.6(2)	132.7(3)
C2–C3–C4 (°)	129.2(2)	128.1(2)	133.0(3)
C$_4$ torsion angle (°)	30.3(4)	27.3(5)	24.6(6)
M1···M2 (Å)	[4.453(1)]	[4.731(1)]	[4.847(1)]

The μ-C$_4$R$_2$H$_2$ moiety can exist as *cis* or *trans* as well as *syn* or *anti* (R groups on same or opposite sides) isomers. Intriguingly, only the *cis-syn* structure was isolated and characterized in each case, and this regioselectivity is corroborated by clean stoichiometric NMR reactions (≥ 90% conversion; Figures S1–S4) for all complexes.[10] These observations are suggestive of a concerted, associative dimerization mechanism for the formation of the C$_4$R$_2$H$_2$ bridge in these complexes, and investigations by DFT calculations have

been performed (see ESI for details). Starting from the monomeric (σ-vinyl)-metalated bis(benzyl) species, contrasting angles of approach and interaction between two M-(σ-vinyl) moieties[11] leads to distinct dimerization pathways and the formation of different μ-C$_4$R$_2$H$_2$ isomers. Taking **Zr$_2$^{H}** as a representation example (Figure S5), the barrier ($\Delta G_{298}^{\ddagger}$ = 31.4 kcal/mol) for the formation of the *cis-syn* dimer is substantially lower than that ($\Delta G_{298}^{\ddagger}$=69.7 kcal/mol) for the *cis-anti* isomer, thus indicating that the former is kinetically favored. For all complexes, the pathway to the *cis-syn* dimer requires significantly lower activation energy than the *cis-anti* form (Table S1; considerations were also given to *trans-syn* [even higher barriers were predicted] and *trans-anti* [no transition state structure was located] pathways), consistent with the observed strong preference for *cis-syn* structures.[12]

Additional discussion and observations concerning the dimerization reaction is pertinent. (1) When the vinyl unit in H$_2$L^R (Scheme 1) was replaced by 1-cyclohexene, reaction with M(CH$_2$Ph)$_4$ afforded the corresponding *mononuclear* [O,N-(σ-cyclohexenyl)] bis(benzyl) complexes (**Ti^{Cy}** and **Zr^{Cy}**; see ESI). Therefore, as expected for the above associative dimerization pathway, such a transformation would be hindered by a substituent at the terminal C(σ-alkenyl) atom. (2) Coates reported that metalation of pyridylamido and phenolate-amine ligands bearing a pendant vinyl group, with group 4 alkyl precursors, both proceeded by intramolecular vinyl insertion and alkyl migration to afford C(sp^3)-chelating catalysts for isoselective α-olefin polymerization.[13] In contrast, the vinyl-containing ligands here manifestly promote facile dimerization of the resultant metalated species. (3) This regioselective transformation is a formally redox-neutral C(sp^2)–C(sp^2) coupling process, which is highly unusual for early transition metals. Related dimerization reactions that are reductive in nature are well-established,[2,14] and reports of non-redox pathways (to afford Ln$_2$,[15] Fe$_2$,[16] and Pt$_2$[17] complexes) are uncommon.

ChemComm

NMR characterization data focusing on the μ-$C_4R_2H_2$ moiety are listed in Table 2 (see Figures S3 and S4 for ^{1}H NMR spectra), and comparisons with η^3-allyl derivatives may be drawn.[18] For $\mathbf{M_2^H}$ complexes bearing the non-coplanar μ-C_4H_4 fragment, J_{HH} couplings of 4–6 Hz between these magnetically inequivalent nuclei are consistent with a *cis*-conformation.[19] Relative to $\mathbf{M_2^H}$, the upfield NMR shift for C_β in the $\mathbf{M_2^{Me}}$ series may be attributed to the dissimilar μ-C_4 coordination apparent from the molecular structures. Bearing in mind differences in electrophilicity, it is surprising that $\mathbf{Zr_2^H}$ and $\mathbf{Hf_2^H}$ (plus $\mathbf{Zr_2^{Me}}$ and $\mathbf{Hf_2^{Me}}$) exhibit closely matched δ_C resonances for the metal-bound $C(sp^2)$ atoms C_α and C_β.[7] In this context, the substantially downfield-shifted NMR peaks for the μ-C_4H_4 fragment in $\mathbf{Ti_2^H}$, and particularly the aromatic-like resonances for C_β and H_β, are noteworthy.[20] While the higher electrophilicity of Ti is a contributing factor, these results imply that this complex is electronically different and may potentially point to a redox non-innocent capability for the μ-C_4H_4 group (especially for reduction-prone metal centers). From a qualitative viewpoint, a combination of μ-*cis*-but-2-ene-1,4-diyl (d^0, d^0) and μ-*cis*-butadiene (d^1, d^1) resonance forms may be employed to describe the μ-$(C_4R_2H_2)$-M_2 bonding.[21]

Molecular orbital (MO) interactions have been analyzed by DFT calculations, and four MOs involving the π orbitals of the C_4 bridge ($\pi_{C_\alpha C_\beta C_\gamma C_\delta}$) and metal d orbitals have been found (Tables S4 and S5 for $\mathbf{M_2^H}$ and $\mathbf{M_2^{Me}}$ respectively). The lowest-energy MO shows bonding across the C_4 unit and is dominated by the $\pi_{C_\alpha C_\beta C_\gamma C_\delta}$ orbital. The second-lowest-energy MO displays bonding for the C_α–C_β and C_γ–C_δ bonds (but antibonding with respect to C_β–C_γ), and in-phase overlap takes place between d_{xy} orbitals and $\pi_{C_\alpha C_\beta}$ (and $\pi_{C_\gamma C_\delta}$). The next MO, which is the HOMO (Table 3 for $\mathbf{Ti_2^H}$), shows bonding for C_β–C_γ (but antibonding with respect to C_α–C_β and C_γ–C_δ), and out-of-phase overlap between d_{xy} orbitals and $\pi_{C_\alpha C_\beta}$ (and $\pi_{C_\gamma C_\delta}$) is evident. The LUMO is antibonding for all three C–C bonds, and contains significant contributions from both d_{xy} and d_{xz} orbitals for the $\mathbf{M_2^H}$ series. On the other hand, the d_{xy} and d_{yz} orbitals contribute to the LUMO for the $\mathbf{M_2^{Me}}$ complexes because of the dissimilar μ-C_4 coordination.

Complexes $\mathbf{Zr_2^{Me}}$ and $\mathbf{Hf_2^{Me}}$ are highly colored and display intense charge transfer absorption bands at λ_{max} 600 and 578 nm ($\varepsilon \sim 1.4 \times 10^3$ dm^3 mol^{-1} cm^{-1}) respectively (Figure S6). An admixture of $\pi_{C_4} \rightarrow d(M)/\pi^*_{py}$ ligand-to-metal and intraligand charge transfer (LMCT and ILCT) is tentatively assigned, in agreement with the calculated MOs (Table S5), and the blue shift from Zr to Hf is entirely consistent with a LMCT transition for d^0 centers. The $\mathbf{Zr_2^H}$ and $\mathbf{Hf_2^H}$ derivatives exhibit absorption shoulders at λ_{max} 400–500 nm that are tentatively assigned to $\pi_{C_4} \rightarrow \pi^*_{py}$ (ILCT) with minor LMCT character. For $\mathbf{Ti_2^H}$, the extremely diffuse nature of the absorption (λ 350–700 nm) is patently different from the $\mathbf{Ti^{Cy}}$ derivative and other complexes.

The results from the X-ray data and DFT calculations allow us to evaluate the μ-$C_4R_2H_2$ structure and M-C_4-M coordination as a function of group 4 metals. The versatility of the delocalized μ-$C_4R_2H_2$ moiety is illustrated by its ability to maintain structural consistency while binding metals of different sizes through variable M–C distances and hapticity.

Table 2 NMR[a] and IR[b] data

$\mathbf{M_2^R}$	C_ω (ppm)	C_α (ppm) [$^1J_{CH}$ (Hz)]	H_α (ppm)	C_β (ppm) [$^1J_{CH}$ (Hz)]	H_β (ppm)	ν_{CC} (cm^{-1})
$\mathbf{Ti_2^H}$	163.84	95.79 [154]	5.27	126.65 [163]	7.12	1592
$\mathbf{Zr_2^H}$	159.75	85.37 [158]	5.36	115.63 [159]	5.56	1593
$\mathbf{Hf_2^H}$	160.53	85.15 [157]	5.04	115.04 [162]	5.61	1594
$\mathbf{Zr_2^{Me}}$	151.58	92.78	–	107.22 [151]	5.10	1591
$\mathbf{Hf_2^{Me}}$	151.06	94.03	–	104.46 [154]	5.13	1591

[a] C_6D_6, 400 (^{1}H)/101 (^{13}C) MHz, 295 K (assigned using [^{1}H,^{13}C]-HSQC, -HMBC, 135-DEPT, COSY and NOESY experiments). [b] Thin film on KBr (ν_{CC} = 1607 and 1606 cm^{-1} for $H_2L^{H,Me}$ respectively).
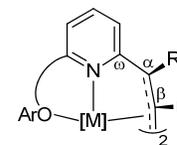
Table 3 Composition of HOMO and LUMO (%; isovalue = 0.03) for $\mathbf{Ti_2^H}$

	HOMO			LUMO		
Composition	d_{xy}	d_{xz}	$\pi_{C_\alpha C_\beta C_\gamma C_\delta}$	d_{xy}	d_{xz}	$\pi_{C_\alpha C_\beta C_\gamma C_\delta}$
$\mathbf{Ti_2^H}$	10.2	2.1	30.2	14.5	38.1	7.4
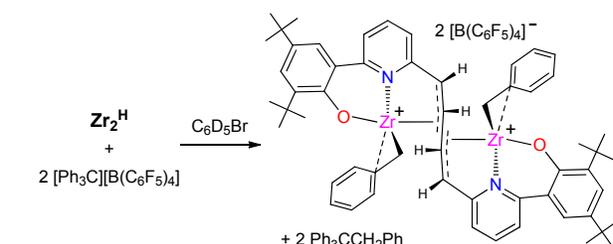
Scheme 2 Reaction of $\mathbf{Zr_2^H}$ with $[Ph_3C][B(C_6F_5)_4]$ in C_6D_5Br.

Next, we endeavored to demonstrate that the μ-$C_4R_2H_2$ core is resistant to electrophilic attack and sufficiently robust to support catalytic reactivity. For example, the treatment of $\mathbf{Zr_2^H}$ with two equivalents of trityl borate $[Ph_3C][B(C_6F_5)_4]$ in C_6D_5Br proceeded cleanly to generate the corresponding dication (containing a η^2-CH_2Ph moiety at each Zr center)[22] and two molecules of Ph_3CCH_2Ph (Scheme 2). The formation of the latter, and the successful

NMR characterization of the dicationic species (Figure S7), confirm that electrophilic attack by Ph_3C^+ does not occur at the μ-C_4 moiety and leads to benzyl abstraction from the Zr sites. In this regard, the reactive nature of the μ-TMM moiety in $[(C_5Me_5)_2Sm]_2[μ-(η^3:η^3)-C(CH_2)_3]$, which undergoes facile C–H activation of toluene, is noted.[4]

Preliminary ethylene polymerization tests in conjunction with trityl borate as cocatalyst have been undertaken,[23] and comparisons with the σ-cyclohexenyl analogues Ti^{Cy} and Zr^{Cy} have been made. Upon activation, the Zr_2^H complex functions as a well-defined catalyst and produces polyethylene (M_n = 2.4 × 10^5) with very narrow M_w/M_n (2.0), while the activity (22 g(polymer) (mmol catalyst)$^{-1}$ h^{-1} atm^{-1}) is modest but nevertheless superior to Zr^{Cy} (< 1 g mmol^{-1} h^{-1} atm^{-1}). Catalyst Zr_2^{Me} is less active (10 g mmol^{-1} h^{-1} atm^{-1}), and both Hf_2 derivatives are inactive. The Ti_2^H catalyst displays enhanced activity (100 g mmol^{-1} h^{-1} atm^{-1}), producing polyethylene with M_n and M_w/M_n values of 1.3 × 10^5 and 2.6 respectively. Interestingly, Ti_2^H is around 5 times more active (per M center) than the mononuclear Ti^{Cy} derivative and produces polyethylene with 2.7 times higher M_n under identical conditions. It has been reported that intermetallic distances in cooperating binuclear catalysts should be relatively short (5.4–5.9 Å for phenoxyiminato-Ti_2 and -Zr_2;[1,24] 3.2–6.5 Å for pyridylamido-Hf_2),[25] in order to facilitate bimetallic enchainment interactions that can lead to enhanced molecular weights. Hence the possibility of bimetallic synergistic effects operating for the Ti_2^H catalyst may be considered, bearing in mind the reasonably close proximity of the Ti_2 centers (4.453(1) Å) and the expected Ti···Ti contraction for the dicationic active species (by analogy to the Zr_2 dication; Figure S8).

In summary, binuclear group 4 complexes supported by a bis-[O,N]-chelating μ-$C_4R_2H_2$ ligand system have been prepared by an unprecedented regioselective, redox-neutral vinylic dimerization reaction, and investigations by X-ray crystallography, various spectroscopic methods and DFT calculations have been undertaken. The delocalized μ-$C_4R_2H_2$ core structure is intriguing because hapticity is readily malleable and different metal sizes can be accommodated, and stability against electrophilic attack is conferred by the chelate effect and the associated steric protection, thus engendering catalytic reactivity (and potential cooperativity) at the bimetallic sites. Further work to broaden the scope of catalytic applications and probe the possibility of bimetallic cooperativity, and synthetic studies to extend to other metal systems, are in progress.

Notes and references

1 M. Delferro and T. J. Marks, *Chem. Rev.*, 2011, **111**, 2450.
2 Y. Shibata, H. Nagae, S. Sumiya, R. Rochat, H. Tsurugi and K. Mashima, *Chem. Sci.*, 2015, **6**, 5394.
3 V. V. Burlakov, P. Arndt, W. Baumann, A. Spannenberg, U. Rosenthal, P. Parameswaran and E. D. Jemmis, *Chem. Commun.*, 2004, 2074.
4 W. J. Evans, T. M. Champagne, J. W. Ziller and N. Kaltsoyannis, *J. Am. Chem. Soc.,* 2006, **128**, 16178.
5 Mononuclear Zr complexes of TMM: (*a*) D. A. Kissounko and L. R. Sita, *J. Am. Chem. Soc.,* 2004, **126**, 5946; (*b*) G. Rodriguez and G. C. Bazan, *J. Am. Chem. Soc.,* 1997, **119**, 343.
6 (*a*) C.-C. Liu and M. C. W. Chan, *Acc. Chem. Res.*, 2015, **48**, 1580; (*b*) M. C. W. Chan, *Chem. Asian J.*, 2008, **3**, 18.
7 (*a*) S. C. F. Kui, N. Zhu and M. C. W. Chan, *Angew. Chem. Int. Ed.*, 2003, **42**, 1628; (*b*) L.-C. So, C.-C. Liu, M. C. W. Chan, J. C. Y. Lo, K.-H. Sze and N. Zhu, *Chem. Eur. J.*, 2012, **18**, 565; (*c*) J. C. Y. Lo, M. C. W. Chan, P.-K. Lo, K.-C. Lau, T. Ochiai and H. Makio, *Organometallics*, 2013, **32**, 449.
8 The Ti_2^{Me} complex could not be synthesized (see ESI).
9 A M–C cutoff distance of ≤ 2.7 Å to assign bonding is applied.
10 NMR reactions (C_6D_6, −30 to 20 ºC) between $M(CH_2Ph)_4$ and H_2L^R resulted in high conversions (≥ 90%) to the *cis*-(*syn*-R_2) products, and the sole identifiable byproduct was toluene.
11 Two-center-two-electron (σ-vinyl)-bridging bimetallic inter-mediates were also considered, but subsequently discounted due to excessive steric hindrance.
12 For *cis*-*syn* structures, the calculated activation energy for the formation of Ti_2^{Me} ($ΔG_{298}^‡$ = 40.1 kcal/mol) was highest amongst the complexes here, consistent with our inability to synthesize this complex.
13 (*a*) J. B. Edson, I. Keresztes, E. B. Lobkovsky and G. W. Coates, *ChemCatChem,* 2009, **1**, 122; (*b*) G. J. Domski, J. B. Edson, I. Keresztes, E. B. Lobkovsky and G. W. Coates, *Chem. Commun.*, 2008, 6137.
14 For example: (*a*) R. Duchateau, A. J. Williams, S. Gambarotta and M. Y. Chiang, *Inorg. Chem.*, 1991, **30**, 4863; (*b*) T. Zippel, P. Arndt, A. Ohff, A. Spannenberg, R. Kempe and U. Rosenthal, *Organometallics*, 1998, **17**, 4429.
15 M. D. Fryzuk, J. B. Love and S. J. Rettig, *J. Am. Chem. Soc.*, 1997, **119**, 9071.
16 M. W. Wallasch, D. Weismann, C. Riehn, S. Ambrus, G. Wolmershäuser, A. Lagutschenkov, G. Niedner-Schatteburg and H. Sitzmann, *Organometallics*, 2010, **29**, 806.
17 W. V. Konze, B. L. Scott and G. J. Kubas, *J. Am. Chem. Soc.*, 2002, **124**, 12550.
18 (*a*) A. Hafner, R. O. Duthaler, R. Marti, G. Rihs, P. Rothe-Streit and F. Schwarzenbach, *J. Am. Chem. Soc.*, 1992, **114**, 2321; (*b*) G. Jiménez Pindado, M. Thornton-Pett and M. Bochmann, *J. Chem. Soc., Dalton Trans.*, 1997, 3115.
19 P. Crews, *J. Am. Chem. Soc.,* 1973, **95**, 636.
20 The downfield shift for $H_β$ should not ascribed to agostic interactions, since the corresponding Ti···H distances are excessive (> 2.9 Å) and a 'normal' $^1J_{CH}$ value (163 Hz) is observed; see: M. Brookhart, M. L. H. Green and L. L. Wong, *Prog. Inorg. Chem.*, 1988, **36**, 1.
21 Natural resonance theory calculations performed on model complexes of M_2^H revealed that the resonance weighting of (d^0, d^0):(d^1, d^1) metal centers increases from Ti to Zr and Hf, thus implying significantly more d^1, d^1 character for the Ti_2^H complex (Tables S2 and S3).
22 The structure of the dication was optimized by DFT calculations. Compared with the molecular structure of Zr_2^H, changes evident in the energy-minimized calculated structure include the hapticity of the μ-C_4H_4 unit (Zr–$C_α$ coordination is significantly stronger) and slight contraction of the Zr···Zr distance (4.52 Å; Figure S8).
23 Conditions: 1.5 μmol of catalyst, $^iBu_3Al/[Ph_3C][B(C_6F_5)_4]$ /catalyst (100/6/1 equiv. respectively), 40 mL of toluene, 1 atm ethylene feed, 20 ºC, 10 minutes.
24 M. R. Salata and T. J. Marks, *J. Am. Chem. Soc.,* 2008, **130**, 12.
25 Y. Gao, A. R. Mouat, A. Motta, A. Macchioni, M. Zuccaccia, M. Delferro and T. J. Marks, *ACS Catal.*, 2015, **5**, 5272.